Helicity-Controlled Liquid Crystal Reaction Field Using Nonbridged and Bridged Binaphthyl Derivatives Available for Synthesis of Helical Conjugated Polymers

Taizo Mori,[†] **Mutsumasa Kyotani,**[‡] **and Kazuo Akagi*,**[†]

Department of Polymer Chemistry, Kyoto University, Kyoto 615-8510, Japan, and Tsukuba Research Center for Interdisciplinary Materials Science (TIMS), University of Tsukuba, Ibaraki 305-8577, Japan

ABSTRACT: The nonbridged and bridged type axially chiral binaphthyl derivatives were synthesized and used as chiral dopants to prepare chiral nematic liquid crystals (N*-LCs) available for an asymmetric reaction field producing helical conjugated polymers. The bridged structure has a linkage between the 2 and 2′ positions of the binaphthyl rings through a tetramethylene chain. It is found that the conformation of the nonbridged binaphthyl derivative in an N-LC solvent is different from that in an isotropic one, giving a different helicity in both solvents, although its configuration remains unchanged. Namely, the nonbridged binaphthyl derivative exhibits transoid (meta-stable) and cisoid (most stable) conformations in N-LC and isotropic solvents, respectively. Meanwhile, the bridged binaphthyl derivative forms a cisoid conformation irrespective of solvent, as expected by the strictly restricted internal rotation of the binaphthyl rings. As a consequence, the nonbridged and bridged binaphthyl derivatives, both of which have an (*R*)-configuration, take a *P*-helicity due to the transoid conformation and an *M*-helicity due to the cisoid one in N-LCs, respectively. This leads to oppositely screwed N*-LCs when these binaphthyl derivatives are added as chiral dopants into N-LCs, though they have the same configuration. Concomitantly, helical polyacetylenes synthesized in the N*-LCs also have oppositely screwed structures in fibril bundles. The usage of the nonbridged and bridged binaphthyl derivatives, as chiral inducers having the same configuration but the opposite helical sense, affords a convenient and promising way to construct the helicity-controlled LC reaction field.

1. Introduction

One of the currently rejuvenated interests on science of chirality is a chiral induction on liquid crystal (LC) through chiral transcription from a chiral compound to an achiral nematic LC (N-LC). It has been elucidated that the chiral nematic LC (N*-LC) or cholesteric LC induced by addition of the chiral compound, as a chiral dopant, into N-LC is available for construction of the asymmetric reaction field which enables us to synthesize helical conjugated polymers.[1] Chiral dopants are mainly employed as chiral center-containing compounds and axially chiral ones.[1–3] The axially chiral binaphthyl derivatives are found to be feasible for control of the helical sense and strength of the N*-LC, especially when they are chemically modified in molecular structure such as introduction of long alkyl chains or mesogenic substituents into the binaphthyl rings.[1–3] Besides, these chiral dopants play an essential role in determining the twisting direction of the helical conjugated polymer and even its spiral morphology synthesized in the N*-LC.[4]

It is well-known that the chiral binaphthyl derivatives are atropisomers, and they are classified into (*R*) [*rectus*; right-handed or clockwise] and (*S*) [*sinister*; left-handed or counterclockwise] configurations, according to a difference in twisting direction of the dihedral angle between the 1,1′ positions of the binaphthyl rings. It seems that the chirality is straightforwardly determined by the twisting direction of the dihedral angle. However, there is some experimental evidence to be taken into account when one judges the chirality. One example is that (*R*)-

(+)-1,1′-bi-2-naphthol and (*R*)-(−)-1,1′-binaphthyl-2,2′-diyl-hydrogenphosphate are dextrorotatory (+) and levorotatory (−), respectively, despite having the same (*R*)-configuration. The former has a nonbridged structure, and the latter has a bridged one linking two oxygen atoms at the 2,2′-positions of the binaphthyl rings via a −P(O)(OH) moiety.[5] Another example is as follows: The mono- and disubstituted crown-ether type binaphthyl derivatives having the same (*R*)-configuration give rise to opposite signs in specific rotation (specific rotatory power), though both of them have the bridged structures.[1f] These experimental facts suggest that the chirality (helicity) of the binaphthyl derivative sensitively depends on the local structure around the 2,2′-positions of the binaphthyl rings, such as bridged structure, and also on the twisting direction and degree of the dihedral angle defined by the binaphthyl rings. Namely, it remains unsolved how both the bridged structure and the change of the dihedral angle affect the helicity of the N*-LC.

In this work, we synthesized the nonbridged and bridged type binaphthyl derivatives, where the latter has a linkage between the 2 and 2′ positions of the binaphthyl rings through a tetramethylene chain. By focusing on these binaphthyl derivatives with the same configuration, we have rationalized why and how they give rise to the N*-LCs with opposite helical twisting directions when used as chiral dopants to N-LCs. Helical polyacetylene synthesized in the N*-LCs thus prepared are examined in terms of the helical screw direction of the fibril bundles by means of measurements with a scanning electron micrograph (SEM) and circular dichroism (CD).

2. Experimental Section

2.1. Synthesis of Chiral Binaphthyl Derivatives. Scheme 1 showed molecular structure of the binaphthyl derivatives. (*R*)- or (*S*)-1,1′-Bi-naphthyl-2,2′-bis-[*para*-(*trans*-4-*n*-penthylcyclohexyl)-

* Corresponding author. E-mail: akagi@star.polym.kyoto-u.ac.jp.
† Department of Polymer Chemistry, Kyoto University.
‡ Tsukuba Research Center for Interdisciplinary Materials Science (TIMS), University of Tsukuba.

Scheme 1. Structures of Nematic Liquid Crystals and Chiral Binaphthyl Derivatives
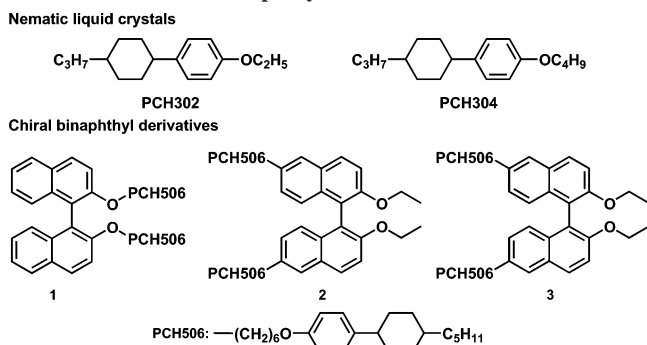
Scheme 2. Synthesis of Bridged Binaphthyl Derivatives with an (R)-configuration
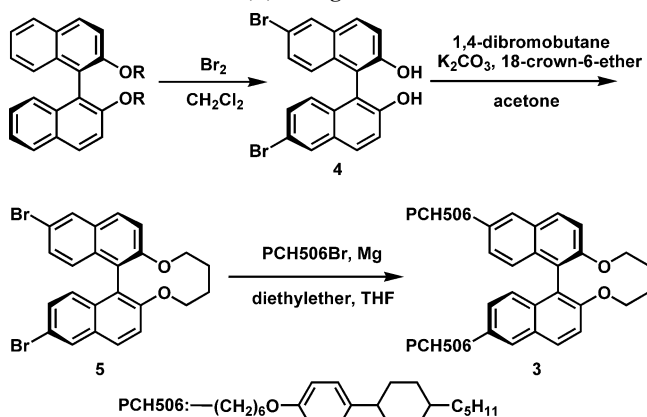
phenolxy-1-hexyl]ether (abbreviated as R-**1** or S-**1**) and (R)- or (S)-6,6′-bis-[*para*-(*trans*-4-*n*-penthylcyclohexyl)phenolxy-1-hexyl]-2,2′-di-ethoxy-1,1′-bi-naphthyl (R-**2** or S-**2**) were synthesized as the nonbridged binaphthyl derivatives. (R)- or (S)-6,6′-Bis-[*para*-(*trans*-4-*n*-penthylcyclohexyl)phenoxy-1-hexyl]-2,2′-butyl-bridged-1,1′-bi-2-naphthol (R-**3** or S-**3**) was synthesized as the bridged binaphthyl derivative.

Synthetic route of the binaphthyl derivative with (R)-configuration (R-**3**) is shown in Scheme 2. Bromination of (R)-(−)-1,1′-bi-2-naphthol in CH₂Cl₂ gave (R)-(−)-6,6′-dibromo-1,1′-bi-2-naphthol (R-**4**) as a white solid in 84% yield.[6] Williamson etherification between R-**4** and 1,4-dibromobutane gave a compound R-**5** as a white solid in 60% yield. Grignard reaction between R-**5** and 1-[*para*-(*trans*-4-*n*-pentylcyclohexyl)phenoxy]-6-bromohexane [PCH506Br] gave R-**3** as a pale yellow solid in 67% yield.[7] Proton (¹H) and carbon (¹³C) nuclear magnetic resonance (NMR) spectra were measured in CDCl₃ using a JEOL 270 MHz NMR spectrometer. Chemical shifts are represented in parts per million down field from tetramethylsilane as an internal standard. Infrared spectra were measured using a JASCO FT-IR 550 spectrometer.

(R)-6,6′-Dibromo-2,2′-butyl-bridged-1,1′-bi-2-naphthol, (R-5). The bridged binaphthyl derivative with (R)-configuration, R-**5**, was synthesized as follows. An amount of 300 mL of acetone was added into a flask containing (R)-(−)-6,6′-dibromo-1,1′-bi-2-naphthol [R-**4**] (1.30 g, 2.9 mmol), K₂CO₃ (0.93 g, 6.8 mmol), and a catalytic amount of 18-crown-6-ether. The solution was refluxed at 60 °C for 2 h. Subsequently, 1,4-dibromobutane (0.65 g, 3.0 mmol) in 50 mL of acetone was added dropwise to the solution at 60 °C. The addition was completed after 6 h, and then the reaction mixture was refluxed at 60 °C for 140 h. The excess K₂CO₃ was filtered off. The crude residue obtained after removal of the solvent was extracted with diethyl ether. The extract was dried with Na₂SO₄. After evaporation of the solvent, the product was purified on a silica gel column (chloroform/*n*-hexane = 1:1). A white solid was obtained in a yield of 0.87 g (60%). Elemental analysis, calcd for C₂₄H₁₈Br₂O₂: C, 57.86; H, 3.64; Br, 32.08. Found: C, 57.57; H,

3.33; Br, 31.42. IR(KBr, cm⁻¹): 3056 (ν_{CH} naphthyl), 2945, 2889 (ν_{CH2}, ν_{CH3}), 1612, 1468 ($\nu_{C=C}$ naphthyl), 1178 (ν_{C-O-C}). ¹H NMR (CDCl₃, δ from TMS, ppm): 7.99 (s, 2H, naphthyl), 7.86, 6.90 (d, 4H, J = 8.9 Hz, naphthyl), 7.45, 7.30 (d, 4H, J = 9.1 Hz, naphthyl), 4.42, 4.07 (4H, J = 11.5 Hz, CH₂O−naphthyl), 1.75 (m, 6H, CH₃). ¹³C NMR (CDCl₃, δ from TMS, ppm): 153.5 (C−O, naphthyl), 132.2, 130.7, 129.8, 129.6, 128.5, 127.1, 121.7, 118.3, 117.8 (naphthyl), 70.4 (CH₂O−naphthyl), 25.4 (CH₃).

(S)-6,6′-Dibromo-2,2′-butyl-bridged-1,1′-bi-2-naphthol, (S-5). The bridged binaphthyl derivative with an (S)-configuration, S-**5**, was synthesized in a similar way to R-**5**. A white solid was obtained in a yield of 0. 91 g (62%). Elemental analysis, calcd for C₂₄H₁₈Br₂O₂: C, 57.86; H, 3.64; Br, 32.08. Found: C, 57.48; H, 3.34; Br, 32.39. IR(KBr, cm⁻¹): 3057 (ν_{CH} naphthyl), 2947, 2839 (ν_{CH2}, ν_{CH3}), 1610, 1474 ($\nu_{C=C}$ naphthyl), 1178 (ν_{C-O-C}). ¹H NMR (CDCl₃, δ from TMS, ppm): 7.99 (s, 2H, naphthyl), 7.82, 6.90 (d, 4H, J = 8.9 Hz, naphthyl), 7.45, 7.22 (d, 4H, J = 9.0 Hz, naphthyl), 4.44, 4.06 (d, 4H, J = 11.5 Hz, CH₂O−naphthyl), 1.75 (m, 6H, CH₃). ¹³C NMR (CDCl₃, δ from TMS, ppm): 153.6 (C−O, naphthyl), 132.3, 130.7, 129.8, 129.6, 128.6, 127.2, 121.8, 118.3, 117.8 (naphthyl), 70.4 (CH₂O−naphthyl), 25.4 (CH₃).

(R)-6,6′-Bis-[*para*-(*trans*-4-*n*-penthylcyclohexyl)phenoxy-1-hexyl]-2,2′-butyl-bridged-1,1′-bi-2-naphthol, (R-3). Magnesium (0.12 g, 4.9 mmol) and 1-[*para*-(*trans*-4-*n*-pentylcyclohexyl)-phenoxy]-6-bromohexane [PCH506Br] (1.39 g, 3.4 mmol) in 3.5 mL of dry diethyl ether were stirred at room temperature until the solution became a suspension. The mixture of (R)-6,6′-dibromo-2,2′-butyl-bridged-1,1′-bi-2-naphthol [R-**5**] (0.48 g, 0.96 mmol), a catalytic amount of 1,3-bis(diphenylphosphino)propane nickel(II) chloride, and dry THF (4 mL) were added into the suspension and then refluxed for 4 h at 40 °C. The reaction was quenched by adding 1 N HCl and water and then extracted with diethyl ether. After drying over Na₂SO₄ and then evaporation of the solvent, the product was purified on a silica gel column (chloroform/*n*-hexane = 1:1). A white solid was obtained in a yield of 0.61 g (67%). Elemental analysis, calcd for C₇₀H₉₂O₄: C, 84.29; H, 9.30. Found: C, 84.62; H, 9.54. IR(KBr, cm⁻¹): 3060 (ν_{CH} phenyl, naphthyl), 2920, 2850 (ν_{CH2}, ν_{CH3}), 1610, 1474 ($\nu_{C=C}$ phenyl, naphthyl), 1176 (ν_{C-O-C}). ¹H NMR (CDCl₃, δ from TMS, ppm): 7.85, 7.43 (d, 4H, J = 8.9 Hz, naphthyl), 7.60 (s, 2H, naphthyl), 7.09, 7.07 (d, 4H, 9.6 Hz, naphthyl), 7.08, 6.80 (d, 8H, 8.7 Hz, phenyl), 4.49, 4.08 (d, 4H, J = 10.0 Hz, CH₂O−naphthyl), 3.90 (t, 4H, J = 6.4 Hz, CH₂O−naphthyl), 2.69 (t, 4H, J = 7.5 Hz, CH−naphthyl) 2.37 (t, 4H, J = 12.0 Hz, CH−Ph), 1.86∼0.86 (m, 36H, CH, CH₂, CH₃). ¹³C NMR (CDCl₃, δ from TMS, ppm): 156.9, 152.3 (C−O, phenyl, naphthyl), 139.7, 138.0, 132.3, 129.8, 128.5, 127.7, 127.3, 126.1, 125.5, 117.3, 114.1, 114.0 (phenyl, naphthyl), 70.2, 67.8 (CH₂O−phenyl, CH₂O−naphthyl), 37.4, 37.3 (CH), 34.6, 33.6, 32.2, 31.2, 29.2, 29.0, 26.6, 26.0, 25.1, 22.7 (CH₂), 14.1 (CH₃).

(S)-6,6′-Bis-[*para*-(*trans*-4-*n*-penthylcyclohexyl)phenoxy-1-hexyl]-2,2′-butyl-bridged-1,1′-bi-2-naphthol, (S-3). The bridged binaphthyl derivative with an (S)-configuration, S-**3**, was synthesized in a similar way to R-**3**. A white solid was obtained in a yield of 0.43 g (98%). Elemental analysis, calcd for C₇₀H₉₂O₄: C, 84.29; H, 9.30. Found: C, 84.56; H, 9.30. IR(KBr, cm⁻¹): 3033 (ν_{CH} naphthyl), 2918, 2845 (ν_{CH2}, ν_{CH3}), 1611, 1467($\nu_{C=C}$ naphthyl), 1177(ν_{C-O-C}). ¹H NMR (CDCl₃, δ from TMS, ppm): 7.85, 7.44 (d, 4H, J = 9.0 Hz, naphthyl), 7.60 (s, 2H, naphthyl), 7.10, 7.07 (d, 4H, 9.6 Hz, naphthyl), 7.08, 6.80 (d, 8H, 8.7 Hz, phenyl), 4.47, 4.06 (d, 4H, J = 10.0 Hz, CH₂O−naphthyl), 3.90 (t, 4H, J = 6.4 Hz, CH₂O−naphthyl), 2.69 (t, 4H, J = 7.5 Hz, CH−naphthyl) 2.39 (t, 4H, J = 12. 0 Hz, CH−Ph), 1.87∼0.87 (m, 36H, CH, CH₂, CH₃). ¹³C NMR (CDCl₃, δ from TMS, ppm): 156.9, 152.3 (C−O, phenyl, naphthyl), 139.7, 138.0, 132.4, 129.8, 128.5, 127.7, 127.4, 127.3, 126.1, 122.2, 117.3, 114.0, 114.0 (phenyl, naphthyl), 70.2, 67.8 (CH₂O−phenyl, CH₂O−naphthyl), 37.4, 37.3 (CH), 34.5, 33.6, 32.1, 31.2, 29.2, 29.0, 26.6, 25.9, 25.1, 22.7 (CH₂), 14.1 (CH₃).

2.2. Measurements of Absorption and CD Spectra of Chiral Binaphthyl Derivatives. Absorption and CD spectra were measured in *n*-heptane using a JASCO J-820 spectrometer. Figure 1 shows the UV−vis and CD spectra of the present nonbridged (R-**1**, R-**2**)
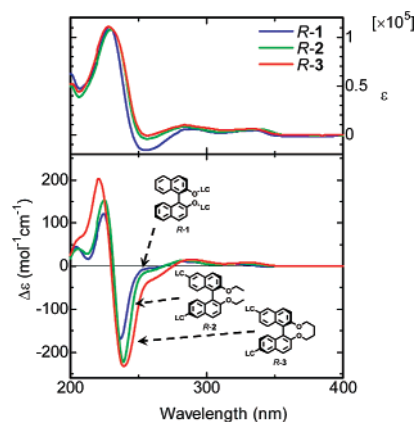
Figure 1. UV−vis and CD spectra of the nonbridged (*R*-**1**, *R*-**2**) and bridged (*R*-**3**) binaphthyl derivatives in *n*-heptane.

and bridged (*R*-**3**) binaphthyl derivatives. In the UV−vis spectra are shown the bands associated with the transitions of the binaphthyl rings: the ^1B_b transition at 200∼250 nm, the ^1L_a transition at 250∼300 nm, the ^1L_b transition at 300∼350 nm. In the CD spectra, the nonbridged (*R*-**1**, *R*-**2**) and bridged (*R*-**3**) binaphthyl derivatives with an (*R*)-configuration show a negative Cotton effect for the ^1B_b transition and intense positive Cotton effects for the ^1L_a and ^1L_b transitions.

2.3. Preparation of N*-LC. N*-LCs were prepared by adding 1.5 mol % of axially chiral binaphthyl derivatives (*R*-**1**, **2**, **3** and *S*-**1**, **2**, **3**) as chiral dopants to the equimolar mixture of N-LCs, 4-(*trans*-4-*n*-propylcyclohexyl)-ethoxybenzene [PCH302] and 4-(*trans*-4-*n*-propylcyclohexyl)-butoxybenzene [PCH304]. The N*-LCs induced by *R*-**1** and *S*-**1**, abbreviated as (*R*-**1**)-LC and (*S*-**1**)-LC, respectively, showed finger-printed textures in the polarizing optical microscope (POM). The microscope observation was carried out under cross nicols by using a Nikon Eclipse E400NIKON ECLIPSE E 400 POL polarizing optical microscope equipped with a Nikon COOLPIX 950 digital camera and a Linkam TH-600PM and L-600 heating and cooling stage with temperature control. Similar finger-printed textures were also observed in the N*-LCs induced by *R*-**2**, *R*-**3**, *S*-**2**, and *S*-**3**. The temperature range of the N* phase was 14∼32 °C in the heating process and −12∼31 °C in the cooling process.

2.4. Synthesis of Helical Polyacetylene in N*-LCs. The N*-LCs thus prepared were used as asymmetric solvents for a Ziegler−Natta catalyst consisting of Ti(O-*n*-Bu)$_4$ and Et$_3$Al. The typical concentration of Ti(O-*n*-Bu)$_4$ was 20 mmol/L, and the mole ratio of [Al]/[Ti] was 4. The N*-LC including the catalyst was aged for 30 min at room temperature. After aging, the N*-LC was moved into a flat-bottom container placed in a Schlenk flask using a syringe. The Schlenk flask was connected to a vacuum line via a flexible joint and then degassed. The acetylene polymerization was carried out by introducing acetylene gas into the catalyst-containing N*-LC. The polymerization temperature was kept constant at 14 °C to maintain the N* phase. The polymerization temperature was controlled by immersing the whole part of the Schlenk flask in a temperature-controlled alcohol bath. The initial acetylene pressure was about 20∼30 Torr and polymerization time was 15∼30 min. After polymerization, the polyacetylene film was washed with purified toluene several times and with a 1 N HCl−methanol mixture and THF under argon at room temperature. The film was dried through vacuum pumping on a Teflon sheet and stored in a freezer at −20 °C.

3. Results and Discussion

3.1. Optical Properties of Chiral Binaphthyl Derivatives.
The binaphthyl derivative has a restricted freedom in internal rotation along the carbon−carbon bond between the 1 and 1′ positions of the binaphthyl rings. The helicity of the binaphthyl derivative therefore depends on the dihedral angle (*θ*) between
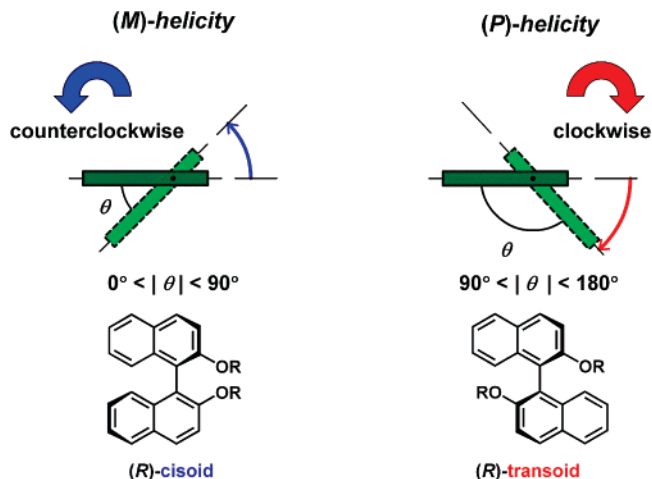

Figure 2. Structures of cisoid and transoid forms of the binaphthyl derivatives with an (*R*)-configuration.

the two binaphthyl rings. For instance, the (*R*)-binaphthyl derivative of the cisoid conformation (0° < *θ* < 90°) and that of the transoid one (90° < *θ* < 180°) have *M*- and *P*-helicity, respectively, as described in Figure 2. It has been clarified so far that the binaphthyl derivatives of *M*- and *P*-helicity induce N*-LCs with counterclockwise and clockwise twisting directions, respectively, when they are added as chiral dopants into a N-LC.[8,9]

The CD spectrum can be interpreted in terms of the exciton coupling theory.[10] The sign and intensity of the CD couplet are related to the value of the dihedral angle (*θ*) between the two binaphthyl rings. The (*R*)-binaphthyl derivatives give a negative couplet for *θ* in the range from 0° to 110° and a positive couplet from 110° to 180°, with negative and positive maxima at 60° and 140°, respectively.[11,12] The values of $\Delta\epsilon$ at approximately 230 nm become larger in the order of the nonbridged *R*-**1** and *R*-**2** and the bridged *R*-**3** binaphthyl derivatives, as shown in Figure 1. Thus, the dihedral angles become smaller in this order. The nonbridged (*R*-**1**, *R*-**2**) and bridged (*R*-**3**) binaphthyl derivatives show positive couplets around 230 nm, indicating *M*-helicity. It is therefore implied that *R*-**1**, *R*-**2**, and *R*-**3** should form cisoid conformations in isotropic solvent like *n*-heptane. It is worthy noting that this argument is supported by the results of the CD spectra of *R*-**1**, *R*-**2**, and *R*-**3** in cyclohexane, one of the isotropic solvents. (See Figure S1 in the Supporting Information.) The positive couplets were also observed in these nonbridged binaphthyl derivatives, confirming the favorableness of the cisoid conformation in an isotropic solvent.

3.2. Characterization of N*-LC.
The helical pitch of the N*-LC was determined using the Cano method,[13] by means of POM under temperature control. The Cano's wedge was warmed up in a hot stage to the preset temperature at the heating rate of 10 °C/min. After time passed enough and it reached the heat equilibrium state, the helical pitch of N*-LC was measured by using the Cano method. The absolute value of the helical twisting power (HTP; β_M), defined as $\beta_M = (pc)^{-1}$, was calculated as the reciprocal of the product between the helical pitch (*p*) and the mole fraction of the chiral dopant (*c*). The concentration of the chiral dopant was 15 mmol %, where the concentrations of PCH302 and PCH304 and the chiral dopant were 100:100:3 in molar ratio, respectively.

Figure 3 shows the temperature dependence of HTP (β_M) of *R*-**1**, *R*-**2**, and *R*-**3**. It is clear that HTP depends on the dihedral angle between the two naphthyl moieties. The HTPs of the nonbridged binaphthyl derivatives (*R*-**1**, *R*-**2**) largely decrease
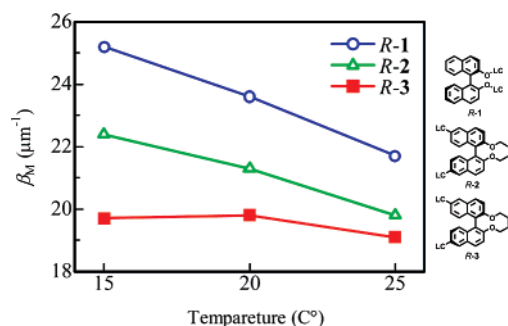
Figure 3. Temperature dependence of helical twisting power (β_M) for the nonbridged (*R*-**1**, *R*-**2**) and bridged (*R*-**3**) binaphthyl derivatives.
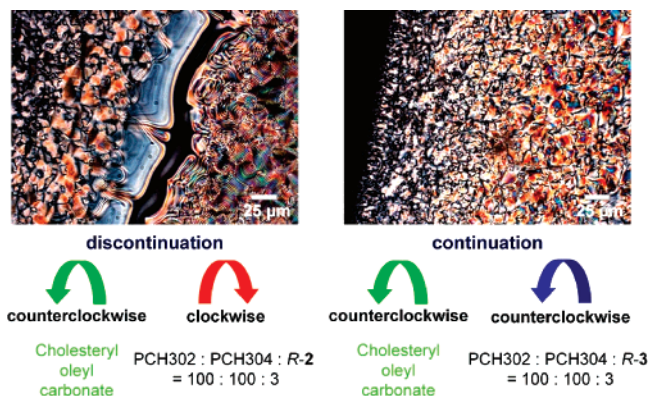

Figure 4. Contact method between the N*-LC induced by *R*-**2** or *R*-**3** and the standard LC, cholesteryl oleyl carbonate of the counterclockwise screw direction.

with increasing temperature. Meanwhile, HTP of the bridged binaphthyl derivative (*R*-**3**) slightly decreases with increasing temperature. This is due to the rigidity between the two naphthyl rings, where the 2 and 2′ positions of the binaphthyl rings are bridged with a tetramethylene chain.

Cholesteryl oleyl carbonate is known to be a counterclockwise N* (cholesteric) LC, and it is useful for the standard LC in the contact method to examine the helical sense of the N*-LC.[14] This method is based on the observation of the mixing area between the N*-LC and the standard LC using POM. When the screw direction of the N*-LC is the same as that of the standard LC, the mixing area will be continuous. Otherwise, it will be discontinuous. As shown in Figure 4, the mixture of (*R*-**1**)-LC or (*R*-**2**)-LC and cholesteryl oleyl carbonate gave the boundary of the Schlieren texture in POM. In contrast, the mixture of (*R*-**3**)-LC and cholesteryl oleyl carbonate showed no change in the optical texture. These results indicate that the screw direction of the (*R*-**1**)-LC or (*R*-**2**)-LC induced by the nonbridged binaphthyl derivative is opposite to that of cholesteryl oleyl carbonate. On the other hand, the screw direction of (*R*-**3**)-LC is the same as that of cholesteryl oleyl carbonate. That is, the screw directions of the (*R*-**1**)-LC and (*R*-**2**)-LC are clockwise, and that of (*R*-**3**)-LC is counterclockwise. Thus, the N*-LC induced by *R*-**1** or *R*-**2** and that by *R*-**3** have opposite screw directions from each other, though the nonbridged (*R*-**1**, *R*-**2**) and bridged (*R*-**3**) binaphthyl derivatives have the same configuration.

Figure 5 show UV−vis and CD spectra of the nonbridged (*R*-**1**, *R*-**2**) and bridged (*R*-**3**) binaphthyl derivatives in N-LC solvent. The nonbridged (*R*-**1**, *R*-**2**) binaphthyl derivatives showed positive Cotton effects in the region of 250 nm, and the bridged (*R*-**3**) one showed a negative Cotton effect. This result implies that the nonbridged (*R*-**1**, *R*-**2**) and bridged (*R*-**3**)
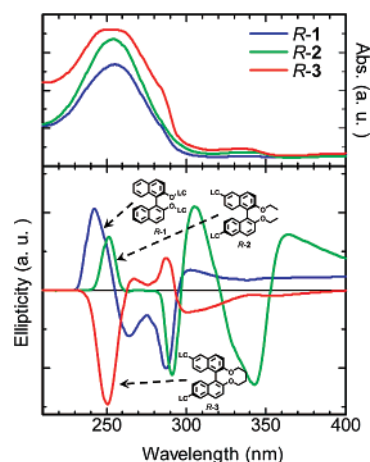

Figure 5. UV−vis and CD spectra of the nonbridged (*R*-**1**, *R*-**2**) and bridged (*R*-**3**) binaphthyl derivatives in LC (PCH302/PCH304 = 1:1) at room temp.

binaphthyl derivatives have different conformations in LCs. Namely, the experimental facts that the nonbridged binaphthyl derivatives (*R*-**1**, *R*-**2**) showed positive Cotton effects and that they showed a clockwise screw direction in LC solvent indicate that they have a *P*-helicity (transoid). On the other hand, the facts that the bridged binaphthyl derivatives (*R*-**3**) showed a negative Cotton effect and that it showed a counterclockwise screw direction in LC solvent indicate that it has an *M*-helicity (cisoid).

3.3. Helical Twisting Directions of Binaphthyl Derivatives. Figure 6 describes stable conformations of the binaphthyl derivatives, obtained by molecular mechanics (MM) calculations.[16] In the nonbridged binaphthyl derivative *R*-**2**, both the cisoid conformation ($\theta = 66°$) and the transoid one ($\theta = 108°$) have almost the same stability. In the bridged binaphthyl derivative *R*-**3**, the cisoid conformation ($\theta = 61°$) is more stable by 21.3 kcal/mol than the *meta*-cisoid one ($\theta = 84°$). The dihedral angle ($\theta = 66°$) of the nonbridged binaphthyl derivative *R*-**2** is larger than that ($\theta = 61°$) of the bridged binaphthyl derivative *R*-**3**.

MM calculations indicated that in the nonbridged binaphthyl derivative *R*-**2**, the stability of the cisoid and transoid conformations is almost equal. In the bridged binaphthyl derivative *R*-**3**, the cisoid conformation is the stable one.[16] Such a difference between the nonbridged and bridged binaphthyl derivatives may cause opposite screw directions of N*-LCs, though they have the same configuration. The nonbridged binaphthyl derivatives (*R*-**1**, *R*-**2**) showed negative Cotton effects in *n*-heptane, while they showed positive Cotton effects in N-LC. This suggests that *R*-**1** and *R*-**2** have cisoid conformations (*M*-helicity) in *n*-heptane, but they have transoid ones (*P*-helicity) in N-LC. As indicated by MM calculations shown in Figure 6, *R*-**2** has two possible conformations, cisoid and transoid ones, where the former is slightly more stable by 2.4 kcal/mol than the latter. It is evident that the cisoid conformation is favorable in isotropic solvent such as *n*-heptane. Nevertheless, although it is not so clear at present, there is a possibility that *R*-**2** takes the *meta*-stable transoid conformation in a specific environment like LC. It might be required for sound understanding to account for entropy effects in molecular interactions between the nonbridged binaphthyl derivatives of the transoid conformation and the surrounding self-assembled LC molecules.

On the other hand, the bridged binaphthyl derivative (*R*-**3**) has strictly restricted freedom in the internal rotation of binaphthyl rings, giving a stable cisoid conformation, as found
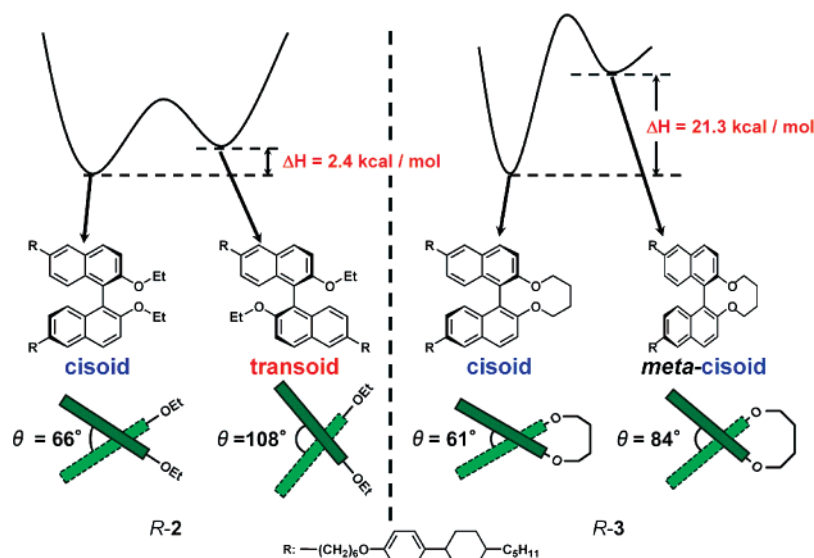
Figure 6. Relative stability of cisoid and transoid forms in the nonbridged [(*R*)-**2**] and bridged [(*R*)-**3**] binaphthyl derivatives.

Table 1. Signs of the Cotton Effects and Screw Directions of the Binaphthyl Derivatives and Helical Polyacetylenes

	Binaphthyl derivatives	CD couplet (in *n*-heptane)	N*-LC		Helical polyacetylene	
			Sign of Cotton effect	Screw direction of N*-LC	Sign of Cotton effect	Screw direction
Nonbridged	*R*-**1**	−	+	clockwise	+	counterclockwise
	R-**2**	−	+	clockwise	+	counterclockwise
Bridged	*R*-**3**	−	−	counterclockwise	−	clockwise
Nonbridged	*S*-**1**	+	−	counterclockwise	−	clockwise
	S-**2**	+	−	counterclockwise	−	clockwise
Bridged	*S*-**3**	+	+	clockwise	+	counterclockwise

in Figure 6. Thus, *R*-**3** shows an *M*-helicity due to the cisoid conformation, resulting in a negative Cotton effect, irrespective of isotropic (*n*-heptane) and anisotropic (N-LC) solvent.

3.4. Morphology of Helical Polyacetylene Films. As shown in Figure 7, polyacetylene films synthesized in (*R*-**1**)-, (*R*-**2**)-LCs, and (*R*-**3**)-LC showed helical fibrillar morphologies with counterclockwise and clockwise directions, respectively. Thus, the nonbridged (*R*-**1**, *R*-**2**) and bridged (*R*-**3**) binaphthyl derivatives give rise to helical polyacetylenes with opposite screw directions to each other, in spite of the fact that both of them have the same chirality.

It should be noted here that the twisting direction of (*R*-**1**)-LC is clockwise, for instance, and the screw direction of helical polyacetylene synthesized under (*R*-**1**)-LC is counterclockwise. The relationship between the screw direction of the helical polyacetylene fibrils and the twisting direction of the N*-LC has been partly rationalized in the previous work[1f] and will be discussed in more detail elsewhere.

Figure 8 shows CD spectra of helical polyacetylene films synthesized in N*-LCs including the nonbridged [(*R*-**2**), (*S*-**2**)-LCs] or bridged [(*R*-**3**), (*S*-**3**)-LCs] binaphthyl derivatives. It is evident that polyacetylene films have Cotton effects in the region from 450 to 800 nm, corresponding to a $\pi \rightarrow \pi^*$ transition of the conjugated polyacetylene chain and that the signs of Cotton effects are opposite to each other between the polyacetylene films synthesized in the N*-LCs including the nonbridged and bridged binaphthyl derivatives. These results are consistent with those of the helical twisted directions of the polyacetylene fibrils observed in SEM photographs, as shown in Figure 7.

Table 1 summarizes signs of Cotton effects and the screw directions of the binaphthyl derivatives, N*-LC and helical polyacetylenes. The chiral dopants, *R*-**1**~*R*-**3**, showed a negative CD couplet (240 nm) in the CD spectra, as shown in Figure 1. This means that the nonbridged (*R*-**1**, *R*-**2**) and the bridged (*R*-**3**) binaphthyl derivatives have the same chirality. However, the N*-LCs induced by the nonbridged binaphthyl derivatives, (*R*-
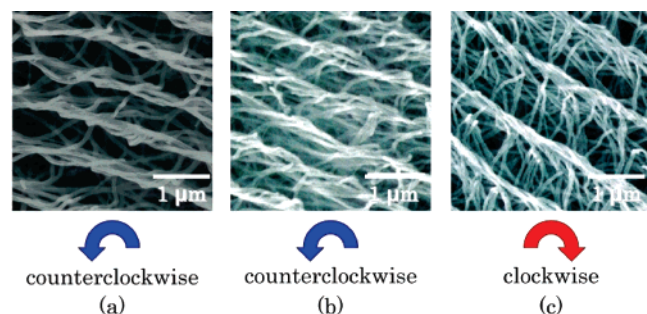
Figure 7. SEM photographs of helical polyacetylene synthesized in (a) (*R*-**1**)-LC, (b) (*R*-**2**)-LC, and (c) (*R*-**3**)-LC.
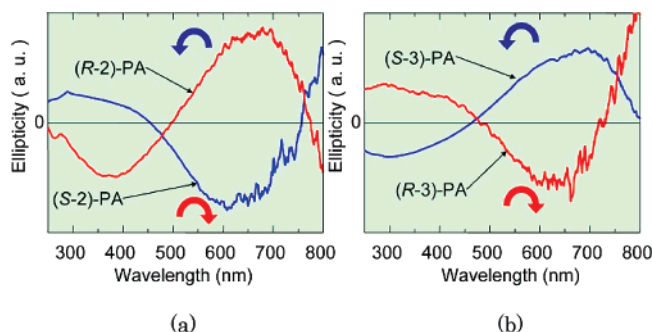

Figure 8. CD spectra of helical polyacetylene films synthesized in (a) (*R*-**2**)-LC and (*S*-**2**)-LC and (b) (*R*-**3**)-LC and (*S*-**3**)-LC.
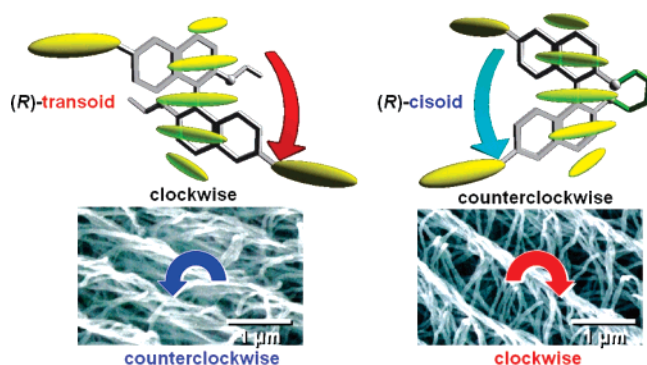

Figure 9. Model structures of the nonbridged (top left) and bridged (top right) binaphthyl derivative with an (*R*)-configuration in N*-LC. The nonbridged and bridged binaphthyl derivatives take the transoid conformation due to *P*-helicity (clockwise) and the cisoid one due to *M*-helicity (counterclockwise) in N*-LC. The SEM images of polyacetylene films synthesized in N*-LC induced by the nonbridged (bottom left) and bridged (bottom right) binaphthyl derivative showed helical fibrillar morphologies with counterclockwise and clockwise directions, respectively.

1) and (*R*-**2**)-LCs, showed clockwise screw directions, which are opposite to that of (*R*-**3**)-LC. As shown in Figure 5, (*R*-**1**) and (*R*-**2**)-LCs showed positive Cotton effects around 250 nm and (*R*-**3**)-LC showed a negative Cotton effect.

CD spectra of helical polyacetylene films synthesized in (*R*-**1**) or (*R*-**2**)-LCs showed positive Cotton effects in the region from 450 to 800 nm. On the other hand, the CD spectrum of a helical polyacetylene film synthesized in (*R*-**3**)-LC showed a negative Cotton effect. Polyacetylene films synthesized in (*R*-**1**)-, (*R*-**2**)-LCs and (*R*-**3**)-LC showed helical fibrillar morphologies with counterclockwise and clockwise directions, respectively. This can be understood by the fact that helical polyacetylene is formed by replicating the screwed structure of N*-LC used as an asymmetric reaction field, and hence the

screwed directions of the helical polyacetylene synthesized in the N*-LCs including the nonbridged (*R*-**1**, *R*-**2**) and bridged (*R*-**3**) binaphthyl derivatives are counterclockwise and clockwise, respectively. This holds also in the case of the chiral dopants of (*S*)-configuration, *S*-**1**~*S*-**3**.

Figure 9 shows structures of the nonbridged and bridged binaphthyl derivative with an (*R*)-configuration in N*-LC and SEM images of the helical polyacetylene synthesized in the N*-LC induced by these binaphthyl derivatives. The nonbridged and bridged binaphthyl derivatives with (*R*)-configuration take the transoid conformation due to *P*-helicity and the cisoid one due to *M*-helicity in N*-LC, respectively. Therefore the N*-LCs induced by these types of binaphthyl derivative show clockwise and counterclockwise screw directions. The screw directions of the N*-LC and helical polyacetylene fibril are opposite to each other, respectively. Namely, it follows that polyacetylene films synthesized in the N*-LC induced by the nonbridged and bridged binaphthyl derivative with an (*R*)-configuration have fibril morphologies with counterclockwise and clockwise screwed directions, respectively.

4. Conclusion

We have synthesized nonbridged and bridged binaphthyl derivatives and used them as chiral dopants to N-LCs. It is found that the conformation of the nonbridged binaphthyl derivative changes between isotropic and N-LC solvents to give a different helicity, although its configuration remains unchanged. Namely, the nonbridged binaphthyl derivative exhibits cisoid (most stable) and transoid (meta-stable) conformations in isotropic and N-LC solvents, respectively. Meanwhile, the bridged one forms a cisoid conformation irrespective of solvent, as expected by the strictly restricted internal rotation of the binaphthyl rings. On the other hand, the stable conformation of the bridged binaphthyl derivatives in isotropic solvents is the same as that in N-LC. As a result, the nonbridged and bridged binaphthyl derivatives with an (*R*)-configuration take on a *P*-helicity due to the transoid conformation and *M*-helicity due to the cisoid one in N-LCs, respectively. This leads to oppositely screwed N*-LCs when these binaphthyl derivatives are added as chiral dopants into N-LCs, though they have the same configuration. Concomitantly, helical polyacetylenes synthesized in the N*-LCs also have oppositely screwed structures in fibril bundles.

These aspects are elucidated by evaluation of the helical sense of the binaphthyl derivatives through signs of Cotton effects and the miscibility test with a standard cholesteric LC and also by observation of the screw direction of helical polyacetylenes synthesized in N*-LCs. At present, it is unclear why the nonbridged binaphthyl derivative forms the meta-stable transoid conformation rather than the most stable cisoid one in N-LC. Nevertheless, the usage of the nonbridged and bridged binaphthyl derivatives, as chiral inducers having the same configuration but the opposite helical sense, affords a convenient and promising way to construct the helicity-controlled LC reaction field.

Supporting Information Available: UV−vis and CD spectra of the binaphthyl derivatives in cyclohexane. This material is available free of charge via the Internet at http://pubs.acs.org.

References and Notes

(1) (a) Akagi, K.; Piao, G.; Kaneko, S.; Sakamaki, K.; Shirakawa, H.; Kyotani, M. *Science* **1998**, *282*, 1683. (b) Akagi, K.; Higuchi, I.; Piao, G.; Shirakawa, H.; Kyotani, M. *Mol. Cryst. Liq. Cryst*. **1999**, *332*, 463. (c) Piao, G.; Akagi, K.; Shirakawa, H. *Synth. Met.* **1999**, *101*, 92. (d) Akagi, K.; Piao, G.; Kaneko, S.; Higushi, I.; Shirakawa, H.; Kyotani, M. *Synth. Met.* **1999**, *102*, 1406. (e) Akagi, K.; Higuchi, I.; Piao, G.; Shirakawa, H.; Kyotani, M. *Mol. Cryst. Liq. Cryst.* **1999**, *332*, 2973. (f) Akagi, K.; Guo, S.; Mori, T.; Goh, M.; Piao, G.; Kyotani, M. *J. Am. Chem. Soc.* **2005**, *127*, 14647.

(2) Sagisaka, T.; Yokoyama, Y. *Bull. Chem. Soc. Jpn.* **2000**, *73*, 191.

(3) Bhatt, J. C.; Keast, S. S.; Neubert, M. E.; Petschek, R. G. *Liq. Cryst.* **1995**, *18*, 367.

(4) (a) Akagi, K. In *Handbook of Conducting Polymers, Conjugated Polymers,* 3rd ed.; Skotheim, T. A., Reynolds, J. R., Eds. CRC Press: New York, 2007; pp 3−14. (b) Goh, M.; Matsushita, T.; Kyotani, M.; Akagi, K. *Macromolecules* **2007**, *40*, 4762. (c) Goh, M.; Kyotani, M.; Akagi, K. *J. Am. Chem. Soc.* **2007**, *129*, 8519.

(5) Jacques, J.; Fouquey, C. *Org. Synth.* **1989**, *67*, 1.

(6) Sogah, G. D. Y.; Cram, D. J. *J. Am. Chem. Soc.* **1979**, *101*, 3035.

(7) Kanazawa, K.; Higuchi, I.; Akagi, K. *Mol. Cryst. Liq. Cryst.* **2001**, *364*, 825.

(8) (a) Ferrarini, A.; Moro, G. J.; Norido, P. L. *Mol. Phys.* **1996**, *87*, 485. (b) Ferrarini, A.; Moro, G. J.; Norido, P. L. *Phys. Rev. E* **1996**, *53*, 681.

(9) (a) Gottarelli, G.; Hibert, M.; Samori, B.; Solladié, G.; Spada, G. P.; Zimmermann, R. *J. Am. Chem. Soc.* **1983**, *105*, 7318. (b) Gottarelli, G.; Spada, G. P.; Bartsch, R.; Solladié, G.; Zimmermann, R. *J. Org. Chem.* **1986**, *51*, 589. (c) Rosini, C.; Franzini, I.; Salvadori, P.; Spada, G. P. *J. Org. Chem.* **1992**, *57*, 6820.

(10) (a) Harada, H.; Nakanishi, K. *Circular Dichroic Spectroscopy Exciton Coupling in Organic Stereochemistry*; University Science Book: Mill Valley, CA, 1983, p 193. (b) Berova, N., Nakanishi, K., Woody, R. W., Eds. *Circular Dichroism: Principles and Application SE*; Wiley-VCH: New York, 2000; p 337. (c) Kitzerow, H.-S., Bahr, C., Eds. *Chirality in Liquid Crystals*; Springer: New York, 2001, p 67. (d) Hanazaki, I.; Akimoto, H. *J. Am. Chem. Soc.* **1972**, *94*, 4102.

(11) (a) DeVoe, H. *J. Chem. Phys.* **1964**, *41*, 393. (b) Zadonmeneghi, M.; Rosini, C.; Salvadori, P. *Chem. Phys. Lett.* **1976**, *44*, 533. (c) Bari, L. D.; Pescitelli, G.; Salvadori, P. *J. Am. Chem. Soc.* **1999**, *121*, 7998.

(12) (a) Mason, S. F.; Seal, R. H.; Roberts, D. R. *Tetrahedron* **1974**, *30*, 1671. (b) Rosini, C.; Rosati, I.; Spada, G. P. *Chirality* **1995**, *7*, 353. (c) Rosini, C.; Superchi, S.; Peerlings, H. W. I.; Meijer, E. W. *Eur. J. Org. Chem.* **2000**, 61.

(13) Gray, G. W.; Mcdonnell, D. G. *Mol. Cryst. Liq. Cryst.* **1979**, *40*, 178.

(14) Heppke, G.; Oestreicher, F. *Mol. Cryst. Liq. Cryst. Lett.* **1978**, *41*, 245.

(15) Kuball. H. G.; Türk, O.; Kiesewalter, I.; Dorr, E. *Mol. Cryst. Liq. Cryst.* **2000**, *352*, 195.

(16) Rappé, A. K.; Casewit, C. J.; Colwell, K. S.; Goddard, W. A., III; Skiff, W. M. *J. Am. Chem. Soc.* **1992**, *144*, 10024.